

# Effects of alternating interactions and boundary conditions on quantum entanglement of three-leg Heisenberg ladder

Qinghui Li<sup>1</sup>, Lizhen Hu<sup>2</sup>, Panpan Zhang<sup>1,3</sup>, Chuanzheng Miao<sup>1</sup>, Yuliang Xu<sup>1</sup>, Zhongqiang Liu<sup>4</sup> and Xiangmu Kong<sup>1\*</sup>

<sup>1</sup>*School of Physics and Optoelectronic Engineering,  
Ludong University, Yantai 264025, China*

<sup>2</sup>*School of Physics and Electronic Engineering,  
Linyi University, Linyi 276000, China*

<sup>3</sup>*Department of physics, Beijing Normal University, Beijing 100875, China and*

<sup>4</sup>*College of Physics and Engineering,  
Qufu Normal University, Qufu, 273165, China*

(Dated: December 31, 2024)

## Abstract

The spin-1/2 three-leg antiferromagnetic Heisenberg spin ladder is studied under open boundary condition (OBC) and cylinder boundary condition (CBC), using the density matrix renormalization group and matrix product state methods, respectively. Specifically, we calculate the energy density, entanglement entropy, and concurrence while discussing the effects of interleg interaction  $J_2$  and the alternating coupling parameter  $\gamma$  on these quantities. It is found that the introduction of  $\gamma$  can completely reverse the concurrence distribution between odd and even bonds. Under CBC, the generation of the interleg concurrence is inhibited when  $\gamma = 0$ , and the introduction of  $\gamma$  can cause interleg concurrence between chains 1 and 3, in which the behavior is more complicated due to the competition between CBC and  $\gamma$ . Additionally, we find that  $\gamma$  induces two types of long-distance entanglement (LDE) in the system under OBC: intraleg LDE and interleg one. When the system size is sufficiently large, both types of LDE reach similar strength and stabilize at a constant value. The study indicates that the three-leg ladder makes it easier to generate LDE compared with the two-leg system. However, the generation of LDE is inhibited under CBC which the spin frustration exists. In addition, the calculated results of energy, entanglement entropy and concurrence all show that there are essential relations between these quantities and phase transitions of the system. Further, we predict a phase transition point near  $\gamma = 0.54$  under OBC. The present study provides valuable insights into understanding the phase diagram of this class of systems.

---

\*Corresponding author. E-mail address: kongxm668@163.com (X. Kong).

## I. INTRODUCTION

As early as 1935, Einstein, Podolsky and Rosen Proposed a special state for two particles (known as the EPR state), commonly referred to as an entangled state, which cannot be written as the direct product of states of two subsystems[1]. Quantum entanglement is the non-local quantum correlation, indicating that it remains unaffected by the distance between the two subsystems and persists regardless of how far apart they are. This concept is vital in quantum mechanics and plays a crucial role in various fields, including condensed matter physics and quantum information science, such as quantum computing, quantum communication, quantum cryptography, etc.[2–9].

Back in 2002, Osterloh et al. investigated the quantum entanglement in one-dimensional XY and Ising models under external magnetic fields. They analyzed the ground state wave function in the critical region and uncovered the connection between quantum entanglement and quantum phase transitions[10, 11]. Following this pioneering work, the study of quantum entanglement in spin systems has garnered increasing interest[12–15]. As is well-known to all, one-dimensional spin systems have computational advantages and can be solved exactly or treated with the renormalization group method. Significant progress has been made in elucidating the relationship between quantum entanglement and phase transitions in these one-dimensional spin systems[16–21].

In the other aspect, spin ladders play a crucial role in explaining the crossover behaviour between one-dimensional and two-dimensional Heisenberg antiferromagnets. These systems can model a class of materials, including  $\text{Sr}_{n-1}\text{Cu}_{n+1}\text{O}_{2n}$ ,  $\text{La}_6\text{Ca}_8\text{Cu}_{24}\text{O}_{41}$  and  $\text{Cu}_2(\text{C}_5\text{H}_{12}\text{N}_2)_2\text{Cl}_4$ , among others[22–24]. In 1996, Dagotto et al. demonstrated that Heisenberg spin ladders with an even number of legs feature energy gaps and exhibit short-range correlations[25]. In contrast, ladders with an odd number of legs lack energy gaps and instead display power-law correlations[26], which is similar to the corresponding spin chains. These theoretical findings have been confirmed in actual materials such as  $(\text{VO})_2\text{P}_2\text{O}_7$  and the cuprate series[27]. Moreover, both experimental and theoretical investigations have revealed fascinating crossover behaviours, such as significant magnetic field effects and dynamic properties[27–31]. Research shows that antiferromagnetic systems, when there is spin frustration and strong quantum fluctuations, manifest unique phenomena[32]. Recently, Almeida et al. used the density matrix renormalization group (DMRG) method and a hard-

core boson mapping technique to investigate the phase diagram of the frustrated Heisenberg ladder under a magnetic field. They gave the conditions for the exchange coupling parameters when there are first-order phase transition lines and bicritical points in the phase diagram[33].

In 2003, Bose designed a mechanism for short-range quantum communication using spin chains as quantum channels[34]. Subsequently, it is proposed that a strong and stable entanglement between two spins that are far away and do not directly interact could be used for long-distance quantum communication. As we all know, in a general short-range interacting system, the pairwise entanglement decays rapidly as the distance between the two spins increases[5, 35]. However, Venuti et al. discovered that the XXX spin chain with alternating interactions exhibits long-distance entanglement (LDE) under open boundary conditions (OBC)[36]. In the experiment, Sahling et al. confirmed the presence of LDE in antiferromagnetic spin chains with alternating interactions for the first time in 2015[37]. This finding has sparked significant interest in the application of alternating interaction spin models within the field of quantum information[38–45]. In 2022, using the DMRG method, we studied the two-leg antiferromagnetic Heisenberg spin system and found that the alternating interactions are conducive to the generation and enhancement of LDE, while the anisotropic interaction inhibits LDE[46].

For the three-leg Heisenberg spin ladder, in the last 20 years, Azzouz et al. calculated the phase diagram and magnetic properties; however, there are few studies on quantum entanglement and quantum correlation[47–51]. In 1996, Frischmuth investigated the magnetic susceptibility and entropy of one-, three-, and five-leg Heisenberg spin ladders under uniform and staggered interactions, respectively, by using the Monte Carlo cycle algorithm and exact diagonalization method[26]. In 2002, Wang studied the ground-state phase diagram of a spin-1/2 frustrated three-leg antiferromagnetic Heisenberg ladder, a symmetric doublet phase and a quartet one were found in the system by the DMRG method[52]. More recently, in 2016, Wang applied the bond mean field method to study the magnetism of a three-leg antiferromagnetic spin-1/2 Heisenberg ladder. They provided the mean-field bond parameters and computed the concurrence values, thereby substantiating the occurrence of phase transitions[53].

In this paper, we investigate the three-leg antiferromagnetic spin-1/2 Heisenberg ladder through the DMRG method, using matrix product states (MPS) as described in

reference[54]. We quantify the dependence of the energy density, entanglement entropy, and concurrence on the interleg interaction  $J_2$  and the alternating coupling parameter  $\gamma$  under OBC and cylinder boundary condition (CBC), respectively. This paper is organized as follows: In Sec. II, we present the Hamiltonian of the system and introduce the DMRG algorithm, calculating the energy of the system when  $\gamma = 0$ ; In Sec. III, we calculate the nearest-neighbour concurrence under the OBC and CBC for  $\gamma = 0$ . In Sec. IV, the effects of  $\gamma$  and CBC on the entanglement of the system are discussed. Sec. V is the conclusion.

## II. MODEL AND ENERGY DENSITY

Consider a three-leg Heisenberg spin ladder with alternating coupling parameter  $\gamma$  (the structure diagram is shown in Fig. 1), and its Hamiltonian can be expressed as

$$H = \frac{1}{4} \left[ \sum_{k=1}^3 \sum_{i=1}^{L-1} J_1 \left( 1 + (-1)^{i+k-1} \gamma \right) \vec{\sigma}_{i,k} \cdot \vec{\sigma}_{i+1,k} + \sum_{k=1}^n \sum_{i=1}^L J_2 \left( \vec{\sigma}_{i,k} \cdot \vec{\sigma}_{i,k+1} \right) \right], \quad (1)$$

where  $\vec{\sigma}_{i,k} = \sigma_{i,k}^x \vec{i} + \sigma_{i,k}^y \vec{j} + \sigma_{i,k}^z \vec{k}$ ,  $\sigma_{i,k}^\alpha$  ( $\alpha = x, y, z$ ) are the Pauli operators on the  $i$ -th site in the chain- $k$ , and the corresponding matrix form in the  $\sigma^z$  representation are

$$\sigma_{i,k}^x = \begin{pmatrix} 0 & 1 \\ 1 & 0 \end{pmatrix}, \quad \sigma_{i,k}^y = \begin{pmatrix} 0 & -I \\ I & 0 \end{pmatrix}, \quad \sigma_{i,k}^z = \begin{pmatrix} 1 & 0 \\ 0 & -1 \end{pmatrix}, \quad (2)$$

in which  $I$  is the imaginary unit.  $L$  is the length of a single chain;  $J_1 > 0$  and  $J_2 > 0$  represent the antiferromagnetic interactions of nearest-neighbour spins along legs (intraleg,  $x$  direction) and rungs (interleg,  $y$  direction), respectively. When  $n = 2$ , the system is in OBC; When  $n = 3$ ,  $\sigma_{i,4}^\alpha = \sigma_{i,1}^\alpha$ , there is an interaction  $J_2$  between the nearest-neighbour spins of the first and third chains, corresponding to CBC in the  $y$  direction of the system, in which the spin frustration exists.  $\gamma = 0$  corresponds to the special case of uniform interactions, and  $0 < \gamma < 1$  corresponds to the case of alternating coupling.  $J_1(1 - \gamma)$  and  $J_1(1 + \gamma)$  describe the "weak bond" and "strong bond", which are shown by the dashed and solid red lines in Fig. 1, respectively.

In this study, we use the DMRG method to calculate the energy and entanglement of the system. It is well known that in this method, any target state  $|\psi\rangle$  can be represented as the superposition form of two subsystems  $|\psi\rangle = \sum_{i,j} c_{i,j} |i\rangle_A |j\rangle_B$ . By applying singular value decomposition, the state can be represented as  $|\psi\rangle = \sum_a \omega_a |\mu_a\rangle_A |\mu_a\rangle_B$ , where  $|\omega_a|^2$

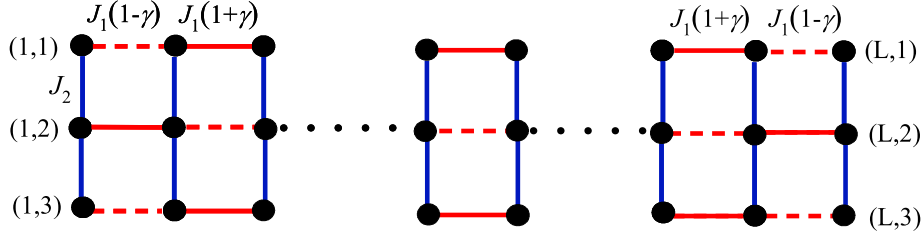


FIG. 1: Schematic diagram of the three-leg alternately coupled spin ladder. The nearest neighbor interactions in the  $x$  direction are alternately strong and weak.

indicates the proportion of the  $|\mu_\alpha\rangle$  in  $|\psi\rangle$ . By preserving at most  $m$  maximum eigenvalues  $\omega_\alpha$  and their corresponding eigenvector  $|\mu_\alpha\rangle$ , the target state can be represented by the truncated state  $|\tilde{\psi}\rangle$ , with the truncation error  $\left| |\psi\rangle - |\tilde{\psi}\rangle \right|^2$ . The ground state is set as the target state, and a maximum of  $m = 400$  states are reserved, which is enough to keep the truncation error  $\sim 10^{-9}$ . In order to avoid the program cannot accurately identify the system when it is in ground state degeneracy, perturbation  $p \left( \sum_i \sigma_i \right)^2$ ,  $p = 0.001$ , is introduced into the Hamiltonian.

In this section, we initially investigate the case of  $\gamma = 0$  under the OBC and CBC (during the calculation that  $J_1 = 1$ ). The energy density of the ground state,  $e_0 = E_0/N$ , as well as the energy densities for the first and second excited states ( $e_1$  and  $e_2$ ), are investigated. Additionally, the energy gaps  $\Delta e_1 = e_1 - e_0$  and  $\Delta e_2 = e_2 - e_0$  are examined as functions of the parameters  $L$  and  $J_2$ , which are shown in Fig. 2. The effects of boundary condition, system size  $L$  and interleg interaction  $J_2$  on them are discussed.

Figure 2(a) illustrates the relation between  $e_0$  and  $L$  for several values of  $J_2$ . As  $L$  increases,  $e_0$  gradually decreases and converges to a stable value. Notably, when  $L > 24$ ,  $e_0$  remains constant, indicating that it is not sensitive to the system size. Therefore, we will use  $L = 24$  for the subsequent calculations. By comparing the variations of  $e_0$  under the two boundary conditions with  $J_2$ , we find that due to spin frustration in the system under CBC, the ground state energy density under OBC is lower than that under CBC, and their difference increases with the increase of  $J_2$ . Additionally, the  $e_0$  gradually decreases with  $J_2$  increases, which indicates that  $J_2$  exerts an inhibition effect on the energy density. In the special case of  $J_2 = 0$ ,  $e_0$  gradually converges to  $1/4 - \ln 2$  as  $L$  increases, which is consistent

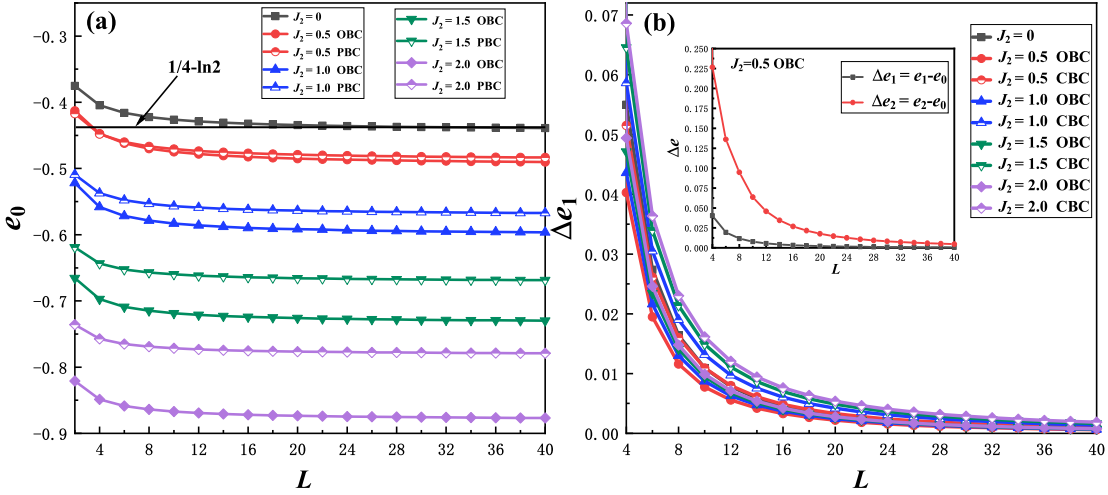


FIG. 2: (a) The variations of the energy density of ground state  $e_0$  with  $L$  for certain values of  $J_2$ , and  $e_0$  gradually converges to a stable value with the increase of  $L$ . (b) The variations of  $\Delta e_1 = e_1 - e_0$  with  $L$  for certain  $J_2$ , showing a trend towards zero as  $L$  increases. The inset gives the variations of  $\Delta e_1$  and  $\Delta e_2 = e_2 - e_0$  with  $L$  for  $J_2 = 0.5$  under the OBC. The full and half-filled symbols correspond to the systems under the OBC and CBC, respectively.

with the result given by Bethe Ansatz method[55].

Figure 2(b) displays the variations of  $\Delta e_1$  with  $L$  for certain  $J_2$ . The value of  $J_2$  has little impact on  $\Delta e_1$ , and  $\Delta e_1$  gradually decreases to zero with the increase of  $L$ , which is consistent with the result that odd-leg ladders have no energy gap[26]. The difference between the energy densities  $e_2$  and  $e_0$  is further studied, and the results are presented in the inset of Fig. 2(b). As an example, under OBC, when  $J_2 = 0.5$ , both  $\Delta e_1$  and  $\Delta e_2$  gradually decrease to zero as  $L$  increases. Through calculations of energy density, we find that the degeneracies of both  $e_1$  and the  $e_2$  are three, indicating that the ground state and first and second excited states are degenerate under the thermodynamic limit, so the degeneracy of the system's ground state is seven.

### III. CONCURRENCE IN HEISENBERG SPIN LADDER

In the previous section, we calculate the energy density of the system. Next, we investigate the entanglement properties when  $\gamma = 0$ , the nearest-neighbor pairwise entanglement

in the ground state is calculated, and the influence of  $J_2$  and boundary condition on the entanglement properties is studied. The pairwise entanglement can be measured by concurrence  $C_{i,j}$ , which represents the entanglement between the  $i$ -th and  $j$ -th sites in a many-body system. The  $C_{i,j}$  can be calculated using the expression[56],

$$C_{i,j} = \max \left\{ \sqrt{\lambda_4} - \sqrt{\lambda_3} - \sqrt{\lambda_2} - \sqrt{\lambda_1}, 0 \right\}, \quad (3)$$

where  $\lambda_k$  ( $k = 1, 2, 3, 4$ ) are the non-negative eigenvalues of  $\rho_{i,j} \tilde{\rho}_{i,j}$  with increasing order, and the reduced density matrix  $\rho_{i,j}$  for the two spins  $i$  and  $j$  can be obtained by tracing out other spins  $\rho_{i,j} = \text{Tr}_{\sigma \neq \sigma_i, \sigma_j} |\psi\rangle \langle \psi|$ ,  $\tilde{\rho}_{i,j} = (\sigma_i^y \otimes \sigma_j^y) \rho_{i,j}^* (\sigma_i^y \otimes \sigma_j^y)$  is the spin-flip density matrix operator of  $\rho_{i,j}$ ,  $\rho_{i,j}^*$  is the complex conjugate of  $\rho_{i,j}$ .

## A. Intraleg entanglement

### 1. Spatial distributions of concurrence

We study the spatial distributions of intraleg concurrence  $C_{i-i+1}$  (where  $C_{i-i+1} \equiv C_{i,i+1}$  are the concurrence of bond between sites  $i$  and  $i + 1$ ,  $i = \text{odd}$  (even) corresponding odd (even) bonds) under two boundary conditions. In the case of OBC, each site in chain- $k$  ( $k = 1$  and  $3$ ) is connected by a single interaction  $J_2$ ; however, each site in chain- $k$  ( $k = 2$ ) is connected by two interactions. Due to the different spin interactions present in each chain, the concurrence behaviour observed in  $k = 2$  is different from that in  $k = 1(3)$ . Under CBC, each site in chain- $k$  ( $k = 1, 2, 3$ ) has the same number of interactions  $J_2$  connecting each site, leading all chains to display similar entanglement properties.

Figure 3 shows the spatial distributions of intraleg concurrence in  $k = 1(3)$  and  $2$  under OBC and CBC with  $L = 24$ , respectively. The results indicate that when  $J_2$  takes a certain value, the concurrence of odd bonds is greater than that of even bonds, leading to a phenomenon known as entanglement separation between odd and even bonds. Despite the uniform interactions among all spins in the chain, the open boundary condition in the x-direction results in an alternating dimerization of concurrence, which enhances the entanglement of odd bonds located near both ends of the chain. Similar phenomena have also been reported in previous literature that studied the spin-1/2 Heisenberg antiferromagnet and XXZ chains[57, 58].



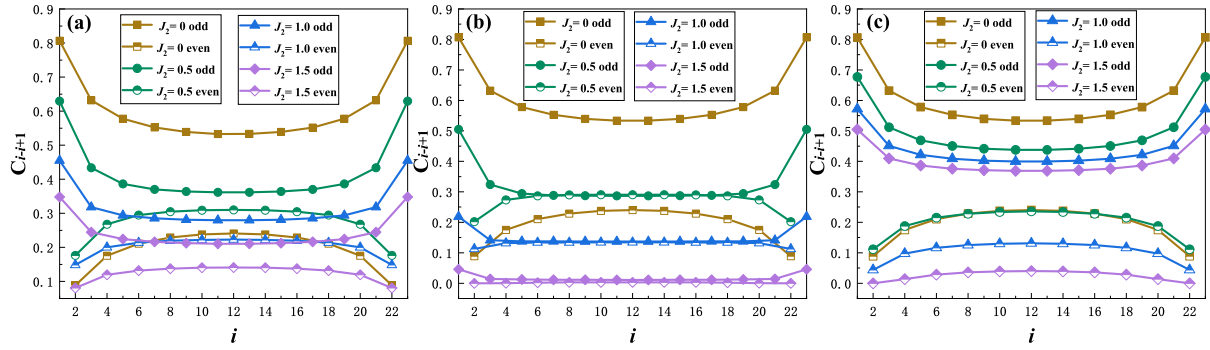


FIG. 3: Spatial distributions of intraleg concurrence with  $L = 24$ . (a) and (b) show the distributions in  $k = 1(3)$  and  $2$  under OBC, respectively. (c) shows the distributions under CBC. There exist the phenomena of entanglement separation between odd and even bonds. The full-filled symbols represent the concurrence on odd bonds, and the half-filled symbols represent the concurrence on even bonds.

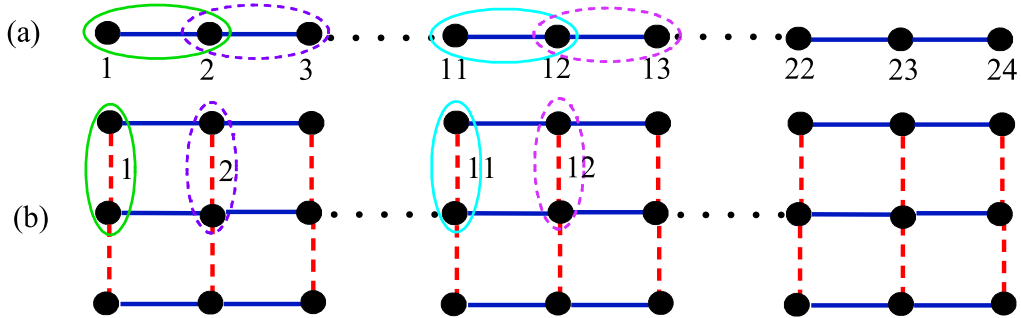


FIG. 4: Schematic diagrams of the bonds studied in the system with  $L = 24$ . (a) Four intraleg bonds: 1-2, 2-3, 11-12, 12-13. (b) Four interleg bonds: 1, 2, 11, 12.

Although the spatial distributions of intraleg concurrence exhibit a similar trend under two boundary conditions, the difference in concurrence between odd and even bonds varies significantly for certain values of  $J_2$ . Taking  $J_2 = 1.5$  as an example, the value of the difference of concurrence between odd and even bonds in the middle of the chain is approximately 0.07 in  $k = 1$ , while it is nearly zero in  $k = 2$  under OBC. It is worth noting that in the case of CBC, this difference becomes more pronounced, indicating that the effect of  $J_2$  on concurrence varies under the two boundary conditions.

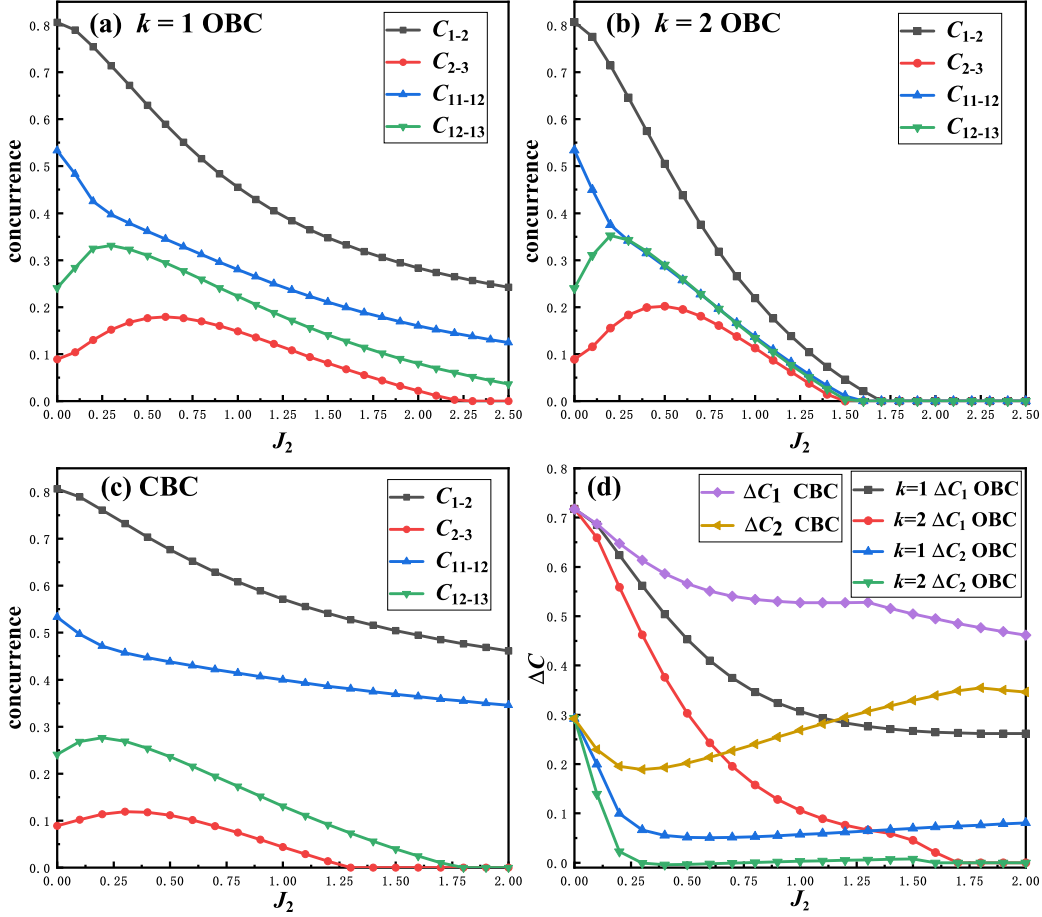


FIG. 5: Relation between concurrence and  $J_2$  among nearest-neighbor spins in the chain,  $L = 24$ : (a) and (b) are the variations of concurrence with  $J_2$  (OBC) of chain-1 and chain-2, respectively. There are two different trends of odd and even bond entanglement. (c) is the variation of concurrence with  $J_2$  (CBC). (d) Variations of the difference between the concurrence of nearest-neighbor bonds with  $J_2$ .

## 2. The effect of $J_2$ on the concurrence

To further investigate the effects of  $J_2$  and boundary conditions on intraleg entanglement, we calculate the concurrence of four typical bonds  $C_{1-2}$ ,  $C_{2-3}$ ,  $C_{11-12}$  and  $C_{12-13}$  (see Fig. 4(a)). It can be observed from Fig.5 that with the increase of  $J_2$ , the concurrence of odd bonds ( $C_{1-2}$  and  $C_{11-12}$ ) gradually decreases, i.e.,  $J_2$  exerts a suppressive effect on concurrence within odd bonds. Meanwhile, the concurrence of the even bonds ( $C_{2-3}$  and  $C_{12-13}$ ) initially increases and

then subsequently decreases. A comparison of the concurrence variations with  $J_2$  reveals that the concurrence of chain-2 rapidly decreases to zero as  $J_2$  increases, indicating that the inhibiting effect of  $J_2$  on concurrence in chain-2 is more pronounced than in chain-1. Additionally, we note that the strength of the concurrence in the odd (even) bonds differs between the two chains, and as  $J_2$  increases,  $C_{1-2}$  and  $C_{11-12}$  of chain-1 consistently remain greater than those in chain-2.  $C_{2-3}$  and  $C_{12-13}$  of chain-2 is larger than those in chain-1 when  $J_2 < 0.75$  and  $0.4$ , respectively, as detailed in Figs. 5(a) and 5(b). The boundary conditions do not affect the variation trend of bond concurrence with  $J_2$ , but the difference between  $C_{11-12}$  and  $C_{12-13}$  under CBC is significantly larger than that under OBC (see Fig. 5(c)).

### 3. *Dimerization of the concurrence*

To delve into the impact of boundary conditions on the dimerization of concurrence, we use the difference in concurrence between nearest-neighbour bonds,  $\Delta C_1 = C_{1-2} - C_{2-3}$  and  $\Delta C_2 = C_{11-12} - C_{12-13}$ , as measures of the concurrence dimerization strength. As depicted in Fig. 5(d), as  $J_2$  increases,  $\Delta C_1$  under OBC and CBC gradually decreases. However, the reduction in  $\Delta C_1$  under CBC is significantly smaller compared to that under OBC, indicating that  $J_2$  plays a suppressive effect on the dimerization effect of the bonds at both ends of the chain. Conversely, the frustration caused by CBC plays a promoting effect on the dimerization effect. Different from  $\Delta C_1$ ,  $\Delta C_2$  initially decreases before increasing as  $J_2$  increases, with this trend being particularly noticeable under CBC. This suggests that the inhibitory effect of  $J_2$  on the dimerization of the central part of the chain transitions from strong to weak. Considering the CBC, the system demonstrates a phenomenon known as spin frustration. The competition between the frustration and  $J_2$  reaches a balance when  $J_2 \approx 0.3$ , and the promotion effect of CBC on the dimerization effect is stronger than the inhibition effect of  $J_2$  when  $J_2 > 0.3$ .

## **B. Interleg entanglement**

In this subsection, we calculate the spatial distribution of interleg concurrence  $C_i$  and the concurrence in four bonds  $C_1$ ,  $C_2$ ,  $C_{11}$  and  $C_{12}$  (corresponding positions in the system with  $L = 24$  are shown in Fig. 4(b)) under OBC (see Fig. 6). Figure 6(a) shows the spatial

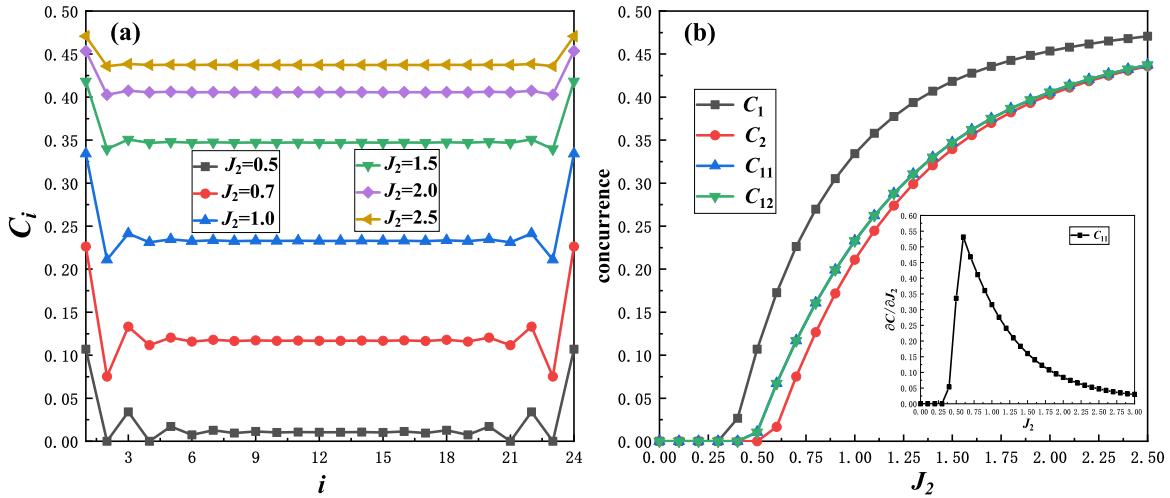


FIG. 6: Interleg concurrence,  $L = 24$ : (a) Spatial distributions of the interleg concurrence. (b) Concurrence of four representative interleg bonds varies with  $J_2$ , which first appears at  $J_2 = 0.2$ . The inset shows the derivative of  $C_{11}$  with respect to  $J_2$ , and there is a maximum value at  $J_2 = 0.6$ .

distribution when  $J_2$  takes several values. Obviously, the concurrence values at both ends are the largest, and the remaining concurrence values are basically in a uniform distribution, and the larger  $J_2$  is, the larger the interleg concurrence is. In Fig. 6(b), when  $J_2$  is small, the interleg concurrence does not exist; when  $J_2$  closes to  $J_{2a} = 0.2$ ,  $C_1$  appears first and then gradually increases.  $C_2$ ,  $C_{11}$  and  $C_{12}$  have similar phenomena to  $C_1$ , but the values of  $J_{2a}$  are different. The inset is the curve of the derivative of  $C_{11}$  with respect to  $J_2$ , in which there is a maximum value of  $C_{11}$  at  $J_2 = 0.6$ .

Additionally, we study the case of CBC and discover that  $C_i$  always remains at zero, i.e., they are in a dead state as  $J_2$  increases. It can be verified that, in this case, the spin frustration phenomenon exists, which inhibits the generation of interleg concurrence.

#### IV. HEISENBERG LADDER WITH ALTERNATING COUPLINGS

The above section, we also calculate the LDE in the case of  $\gamma = 0$ . The findings indicate that LDE (e.g., concurrence between sites 1 and  $L$  in chain-1) is zero in this case. Previous study has shown that the introduction of  $\gamma$  is conducive to the generation of LDE, which can introduce more abundant entanglement phenomena into the system[46]. In this section,

considering OBC, we investigate the influence of  $\gamma$  on the system's energy, entanglement entropy and concurrence, especially LDE, and further discuss the relation between quantum entanglement and quantum phase transitions (during calculation that  $J_2 = J_1 = 1$ ).

According to the DMRG method, the whole system is divided into system block A and environment block B. For a quantum system containing two subsystems A and B, the Von Neumann entropy[59, 60] is defined as the partial entanglement entropy of two subsystems A or B[61],

$$S = S(\rho_A) = S(\rho_B) = -\text{Tr}(\rho_A \log \rho_A) = -\text{Tr}(\rho_B \log \rho_B) = -\sum_i \lambda_i \log \lambda_i, \quad (4)$$

where  $\rho_A = \text{Tr}_B(\rho_{AB})$ ,  $\rho_B = \text{Tr}_A(\rho_{AB})$ ,  $\rho_{AB} = \rho$  is the ground state density matrix of the system,  $\lambda_i$  is the nonzero eigenvalue of  $\rho_A$  or  $\rho_B$ .

### A. Energy density and entanglement entropy

Without loss of generality, similar to the Sec. II, we calculate the energy density  $e_0$ , first excited state energy density  $e_1$  and their difference  $\Delta e_1$ , which vary with  $L$  and  $\gamma$  (see Fig. 7). From Fig. 7(a), we find that  $e_0$  gradually decreases and converges to a stable value with the increase of  $L$ . Compared to the case when  $\gamma = 0$ , the convergence rate of  $e_0$  to the stable value decreases with the increase of  $L$  due to the introduction of  $\gamma$ . For small values of  $\gamma$ ,  $e_0$  essentially converges when  $L = 28$ , but for larger values of  $\gamma$ , the convergence rate of  $e_0$  is slower. As an example, we fit the data in Fig. 7(a) when  $\gamma = 0.9$  and get the relation between  $e_0$  and  $L$ ,  $e_0 = 0.358\exp(-L/2.715) + 0.124\exp(-L/12.352) - 0.738$ . When  $L \rightarrow \infty$ ,  $e_0 = -0.738$ . According to the data of Fig. 7(a), when  $\gamma = 0.9$  and  $L = 28$ ,  $e_0 = -0.726$ , which is near  $-0.738$ . In order to study the phase transition, it is necessary to calculate the case of  $L \rightarrow \infty$ . For convenience, the system with  $L = 28$  is chosen to calculate the entanglement in the next subsection.

Next, we study the influence of  $\gamma$  on the system energy and entanglement entropy (see Figs. 7(b) - (d)). In Fig. 7(b), it is observed that when  $L$  takes several values,  $\Delta e_1$  first decreases with the increase of  $\gamma$ , then slightly increases around  $\gamma = 0.54$ , and subsequently drops to zero. Figure 7(c) indicates that with the increase of  $\gamma$ , there are two minimum values of the second derivative of  $e_0$  at  $\gamma = 0.04$  and  $0.56$ . Figure 7(d) shows that the  $S$  varies with  $\gamma$  when  $L$  takes different values, and the analysis reveals that there are two peaks

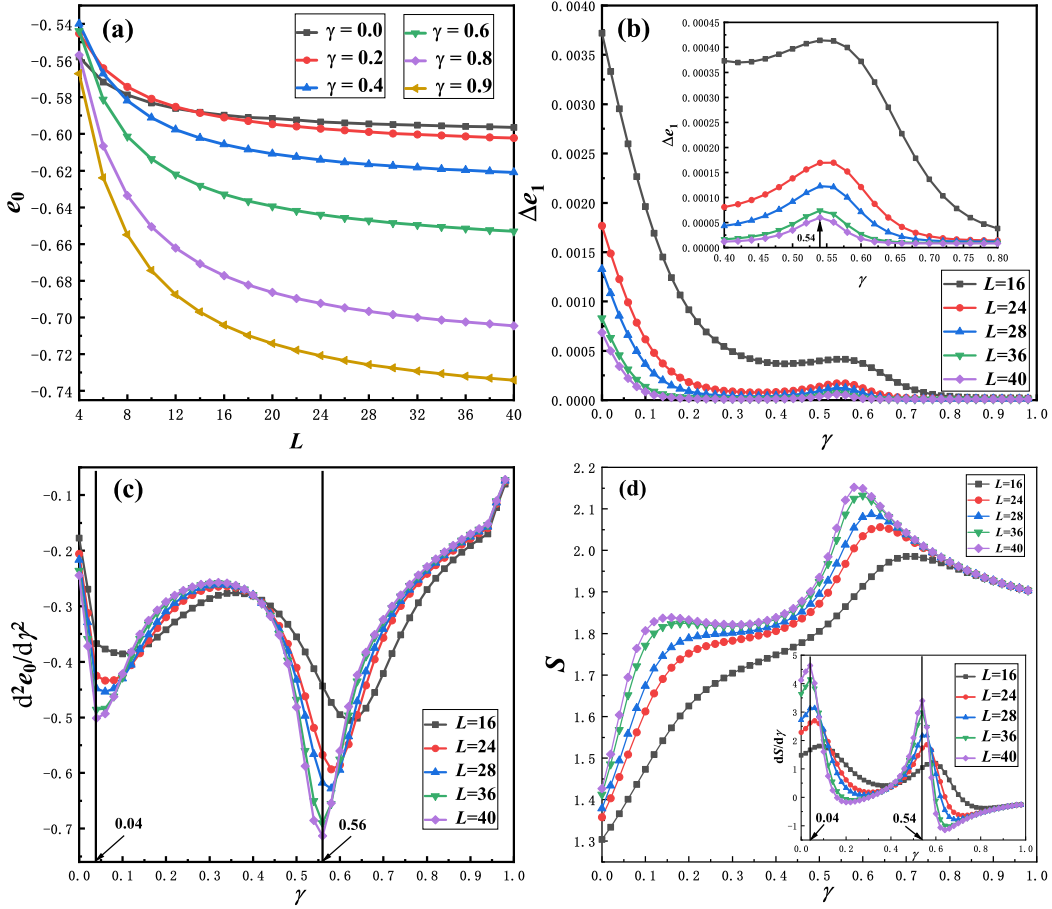


FIG. 7: Ground state energy density  $e_0$ , energy gap  $\Delta e_1$  and entanglement entropy  $S$ : (a)  $e_0$  gradually decreases and converges to a stable value with the increase of  $L$ . (b) Variations of  $\Delta e_1$  with  $\gamma$  for  $L = 16, 24, 28, 36, 40$ , where there is a small peak near  $\gamma = 0.54$  when  $L = 40$ . (c) The second derivative of  $e_0$  with respect to  $\gamma$ . (d) There are two peaks in the variations of  $S$  with  $\gamma$ . The inset shows the first derivative of  $S$  with respect to  $\gamma$ .

of  $S$  with the increase of  $\gamma$ , and the larger  $L$  is, the more obvious the peak values are. The inset in Fig. 7(d) shows that with the increasing  $L$ , there are two maximum values of the derivative of  $S$  at  $\gamma = 0.04$  and  $0.54$ , respectively.

Based on the above analysis of energy density gap and entanglement entropy, we predict that there are two phase transition points at about  $\gamma = 0.04$  and  $0.54$  in the system.

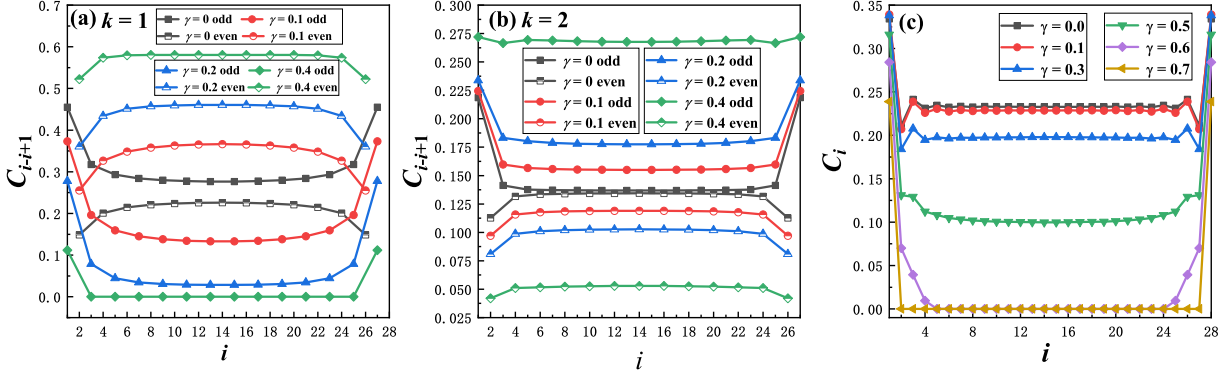


FIG. 8: Intraleg and interleg concurrence spatial distributions ( $L = 28$ ,  $J_1 = J_2 = 1$ ). (a) and (b) are the spatial distributions of nearest-neighbour concurrence of chains-1 and 2 when  $\gamma = 0, 0.1, 0.2, 0.4$ , and the distributions of concurrence reverse the separation of odd and even bonds when  $\gamma > 0$ , where the full-filled symbol represents concurrence on odd bonds, the half-filled symbol represents concurrence on even bonds. (c) is the spatial distribution of interleg concurrence between chains-1(3) and 2 when  $\gamma = 0, 0.1, 0.3, 0.5, 0.6, 0.7$ .

## B. Effect of $\gamma$ on entanglement

This subsection investigates the effect of  $\gamma$  on intraleg and interleg concurrence by calculating the spatial distribution of the nearest-neighbour spins concurrence in chain-1(3) and 2, along with the variations of  $C_1$ ,  $C_2$ ,  $C_{13}$  and  $C_{14}$  with  $\gamma$  when  $L = 28$ .

### 1. spatial distributions of nearest-neighbor concurrence

In Sec. III A, we have obtained that when  $\gamma = 0$ , due to the influence of the OBC in the  $x$  direction of the system, the phenomenon of odd and even bond separation appears in the intraleg concurrence. Figures 8(a) and (b) show the spatial distribution of nearest-neighbor entanglement  $C_{i-(i+1)}$  when  $\gamma$  takes several values. It can be seen that introducing  $\gamma$  (when  $J_1 = J_2 = 1$ , this problem can be seen as the competition between  $\gamma$  and OBC) makes the concurrence of odd and even bonds in chain-1 gradually weaken and strengthen, respectively. In contrast to the intraleg concurrence, the interleg concurrence distribution across the rungs exhibits greater uniformity. Figure 8(c) shows that due to the influence

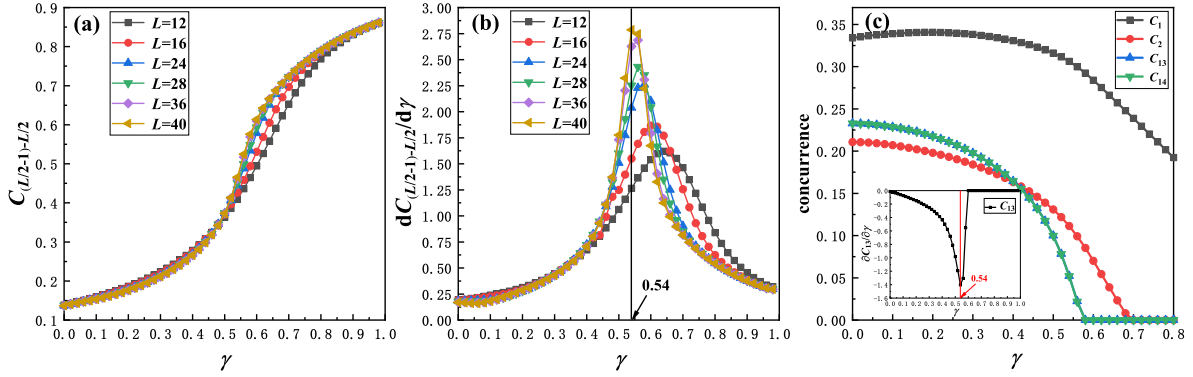


FIG. 9: (a) Concurrence of the "strong bonds"  $C_{(L/2-1)-L/2}$  in the middle of the chain varies with  $\gamma$  for different system sizes  $L$ . (b) Variation of the derivative of  $C_{(L/2-1)-L/2}$  with respect to  $\gamma$  in chain-2. With the increase of  $L$ , the value of  $\gamma$  gradually tends to 0.54 when  $dC_{(L/2-1)-L/2}/d\gamma$  reaches the maximum value. (c) The relation between the concurrence of the four transverse bonds and the  $\gamma$  for  $L = 28$ . The inset shows the derivative of  $C_{13}$  with respect to  $\gamma$ , where there is a minimum at  $\gamma = 0.54$ .

of boundary conditions, the interleg concurrence at both ends,  $C_1$  and  $C_{28}$  is larger than  $C_{14}$  at the middle of the ladder. In addition, the concurrence values in the middle of the chain are nearly identical, indicating that the dimerization effect brought by OBC only affects the concurrence of a few bonds at both ends. As can be seen from Fig. 8(c), the interleg concurrence has reached a uniform distribution in the middle of the ladder, i.e.,  $C_{13} = C_{14} = C_{15}$ .

## 2. Further verification of phase transition point

In order to further study the relation between quantum entanglement and phase transitions of the system, we calculate the concurrence  $C_{(L/2-1)-L/2}$  of the "strong bonds" at the centre of chain-2 (this selection is made to minimize the boundary effects), and discuss the dependence of  $C_{(L/2-1)-L/2}$  on  $\gamma$  for different system sizes  $L$  (see Figs. 9(a) and (b)).

Figure 9(a) shows the function of the  $C_{(L/2-1)-L/2}$  in chain-2 with  $\gamma$  for different  $L$  values. The results indicate that the concurrence monotonically increases with  $\gamma$  and remains largely independent of the system size  $L$  (which means that the concurrence is insensitive to  $L$ ) for



$\gamma \leq 0.5$  and  $\gamma \geq 0.9$ ; when  $0.5 < \gamma < 0.9$ , the concurrence increases with  $L$ . A notable feature is the presence of a maximum in the first derivative of  $C_{(L/2-1)-L/2}$  with respect to  $\gamma$ , as shown in Fig. 9 (b). It is important that as  $L \rightarrow \infty$ , the extreme point  $\gamma = 0.54$  is close to the predicted phase transition point.

To further discuss the influence of  $\gamma$  on interleg concurrence, the  $C_1$ ,  $C_2$ ,  $C_{13}$  and  $C_{14}$  are studied for  $L = 28$  (see Fig. 9(c)). The results indicate that  $C_{13}$  and  $C_{14}$  gradually decrease to zero at  $\gamma = 0.54$ . In contrast,  $C_1$  persists for a larger  $\gamma$  value before diminishing to zero, a behaviour attributed to the dimerization effect. The inset in Fig. 9(c) is the derivative of the middle bond concurrence  $C_{13}(C_{14})$ , in which there is a minimum value near  $\gamma = 0.54$ , which corresponds to the predicted phase transition point.

### C. Long-distance entanglement

Next, we investigate the LDE within the system. After calculation, one finds that there are two types of LDE in this system,  $C_L^1$  and  $C_L^2$ .  $C_L^1$  is the entanglement between sites 1 and  $L$  in  $k = 1(3)$ , and  $C_L^2$  is the entanglement between site 1 in  $k = 1(3)$  and site  $L$  in  $k = 3(1)$ .

Figure 10(a) demonstrates that both  $C_L^1$  and  $C_L^2$  tend to be stable with the increase of  $L$  and converge completely at  $L = 28$ , which indicates that LDE is not sensitive to  $L$ . Consequently, high-intensity entanglement can still be obtained in an infinite system. Comparing  $C_L^1$  and  $C_L^2$ , one finds that when  $L$  is very small, the two kinds of LDE reach the same strength. It is indicated that for the ladder structure, the difference between the two kinds of LDE gradually decreases to zero with the increase of  $L$ , which can be easily seen from the ladder structure.

Figure 10(b) shows the variation of  $C_L^1$  with  $\gamma$  and the convergence with the system size  $L$ . The result reveals that, due to the influence of the interleg coupling  $J_2$ , the two-leg ladder requires a larger  $\gamma$  value to generate LDE compared to a single spin chain. Our calculations indicate that the three-leg ladder necessitates a smaller  $\gamma$  value for LDE to generate in comparison to the two-leg ladder. Taking  $L = 16$  as an example, the LDE in the two-leg ladder appears at about  $\gamma = 0.51$ , while  $\gamma = 0.46$  for the three-leg ladder. There is a maximum value of the first derivative of  $C_L^1$  with respect to  $\gamma$  in the inset. As  $L \rightarrow \infty$ , the extreme point value  $\gamma = 0.58$  is near the critical point of the quantum phase transition.

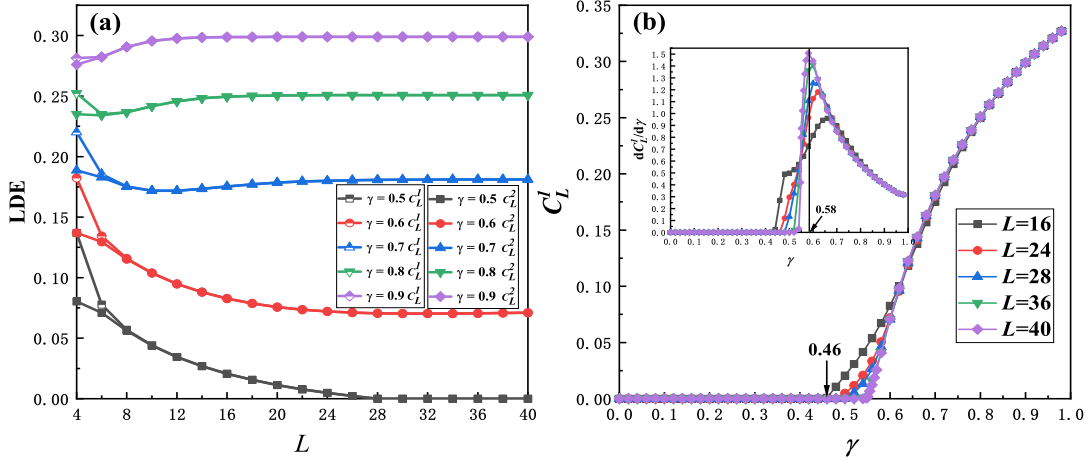


FIG. 10: (a) The LDE,  $C_L^1$  and  $C_L^2$  versus  $L$  for different values of  $\gamma$ , which reach the same intensity as  $L$  is small. (b)  $C_L^1$  and its derivative with respect to  $\gamma$  for different values of  $L$ . The inset shows the variation of the derivative of  $C_L^1$  with respect to  $\gamma$ , in which there is a maximum value at  $\gamma = 0.58$  as  $L \rightarrow \infty$ .

#### D. Effect of spin frustration on entanglement

As established in the previous section, for the system with the OBC,  $\gamma$  can give rise to LDE. However, we find that  $\text{LDE} = 0$  in the system with CBC, which can be interpreted as due to spin frustration that exists in the system under CBC. Here, we will further study the effect of spin frustration in the system on nearest-neighbor entanglement.

In Sec. III B, we already know there is no interleg concurrence in the system with  $\gamma = 0$  and CBC. However, the calculation in the case of CBC shows that  $\gamma$  can cause concurrence between chains-1 and 3. This phenomenon arises because the distributions of intraleg spin interactions in chains-1 and 3 are identical (see Fig. 1). As an example, we study the distribution of the interleg concurrence  $C_i$  and the variations of  $C_1$ ,  $C_2$ ,  $C_{13}$  and  $C_{14}$  with  $\gamma$  (as shown in Fig. 11).

Due to the dimerization effect brought by OBC in the  $x$  direction,  $C_1$  and  $C_{28}$  is the strongest at both ends of the ladder, and the concurrence of odd and even bonds changes with the position  $i$ , and it decreases to zero as  $i \rightarrow 14$ . The even bond concurrence is very small and almost always zero. As the increase of  $\gamma$ , except for the concurrence of the odd

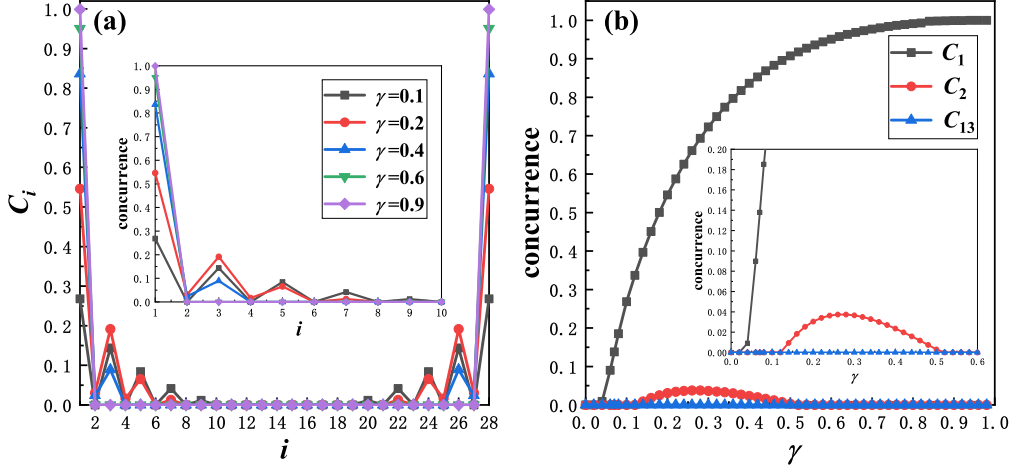


FIG. 11: Interleg concurrence between chains-1 and 3,  $L = 28$ : (a) The spatial distribution of interleg concurrence. (b) The concurrence of the four interleg bonds varies with  $\gamma$ ,  $C_1$  and  $C_2$  are generated when  $\gamma = 0.04$  and  $0.12$ , respectively, and  $C_{13}$ ,  $C_{14}$  are always zero.

bonds at the most ends of the ladder, the concurrence of the remaining bonds eventually decreases to zero, and  $C_{13}$  and  $C_{14}$  of the middle interleg bonds are always zero. For small values of  $\gamma$ ,  $C_i = 0$ , a consequence of the suppressive influence of frustration on interleg concurrence. With the increase of  $\gamma$ ,  $C_1$  is generated at  $\gamma = 0.04$  and then increases rapidly. It is easy to see that  $\gamma$  is conducive to the generation of entanglement of odd bonds at the most ends of the ladder. Unlike  $C_1$ ,  $C_2$  begins to appear at  $\gamma = 0.12$ , increases and then decreases as  $\gamma$  increases, and disappears at  $\gamma = 0.52$ .

## V. CONCLUSION

In this study, we investigate the spin-1/2 three-leg antiferromagnetic Heisenberg ladder under OBC and CBC by calculating the dependence of the energy density, entanglement entropy and concurrence on the interleg interaction  $J_2$  and the alternation parameter  $\gamma$ . In the case of OBC, as  $\gamma = 0$ , it is found that entanglement separation of odd and even bonds occurs in the system. The introduction of  $\gamma$  can completely reverse the distribution of concurrence between odd and even bonds. Additionally,  $\gamma$  can induce the emergence of two types of LDE, i.e., the intraleg LDE and the interleg one. The results show that the

three-leg ladder makes it easier to produce LDE than the two-leg system and makes the physical mechanism and properties of LDE clearer, which is conducive to obtaining stable entangled states effectively in experiments. We also find that the nearest-neighbor spins entanglement, entanglement entropy, energy gap and LDE are essentially related to phase transitions, and a phase transition point near  $\gamma = 0.54$  is predicted by calculating.

Finally, the effect of CBC on entanglement is discussed, revealing that LDE production is inhibited in the spin frustration. When  $\gamma = 0$ , the interleg concurrence is always in a dead state, and  $\gamma$  can lead to interleg concurrence appearing between chains-1 and 3.

## VI. ACKNOWLEDGEMENTS

This work is supported by the Shandong Provincial Natural Science Foundation, China, under Grant No. ZR2022MA041, and No. ZR2021ME147; National Natural Science Foundation of China under Grants No. 11675090, and No. 11905095; Innovation Project for graduate students of Ludong University IPGS2024-049.

- 
- [1] A. Einstein, B. Podolsky, N. Rosen, Can quantum-mechanical description of physical reality be considered complete? *Phys. Rev.* **47** (1935) 777.
  - [2] M.A. Nielsen, I.L. Chuang, *Quantum Computation and Quantum Information*, Cambridge University Press, Cambridge, 2000.
  - [3] R. Horodecki, P. Horodecki, M. Horodecki, K. Horodecki, Quantum entanglement, *Rev. Mod. Phys.* **81** (2009) 865.
  - [4] T. Nishioka, Entanglement entropy: Holography and renormalization group, *Rev. Mod. Phys.* **90** (2018) 035007.
  - [5] L. Amico, R. Fazio, A. Osterloh, V. Vedral, Entanglement in many-body systems, *Rev. Mod. Phys.* **80** (2008) 517.
  - [6] D. Boschi, S. Branca, F. De Martini, L. Hardy, S. Popescu, Experimental realization of teleporting an unknown pure quantum state via dual classical and Einstein-Podolsky-Rosen channels, *Phys. Rev. Lett.* **80** (1998) 1121.

- [7] N. Gisin, G. Ribordy, W. Tittel, H. Zbinden, Quantum cryptography, *Rev. Mod. Phys.* **74** (2002) 145.
- [8] C.H. Bennett, G. Brassard, C. Crépeau, R. Jozsa, A. Peres, W.K. Wootters, Teleporting an unknown quantum state via dual classical and Einstein-Podolsky-Rosen channels, *Phys. Rev. Lett.* **70** (1993) 1895.
- [9] O. Hirota, A.S. Holevo, C.M. Caves, *Quantum Communication, Computing, and Measurement*, Plenum Press, New York, 1997.
- [10] A. Osterloh, L. Amico, G. Falci, R. Fazio, Scaling of entanglement close to a quantum phase transition, *Nature* **416** (2002) 608-610.
- [11] F.G.S.L. Brandão, M. Horodecki, An area law for entanglement from exponential decay of correlations, *Nat. Phys.* **9** (2013) 721-726.
- [12] M. Kargarian, R. Jafari, A. Langari, Dzyaloshinskii-Moriya interaction and anisotropy effects on the entanglement of the Heisenberg model, *Phys. Rev. A* **79** (2009) 042319.
- [13] S.-J. Gu, S.-S. Deng, Y.-Q. Li, H.-Q. Lin, Entanglement and quantum phase transition in the extended hubbard model, *Phys. Rev. Lett.* **93** (2004) 086402.
- [14] J. Ren, Y.-M. Wang, W.-L. You, Quantum phase transitions in spin-1 XXZ chains with rhombic single-ion anisotropy, *Phys. Rev. A* **97** (2018) 042318.
- [15] F.-W. Ma, S.-X. Liu, X.-M. Kong, Quantum entanglement and quantum phase transition in the XY model with staggered Dzyaloshinskii-Moriya interaction, *Phys. Rev. A* **84** (2011) 042302.
- [16] M. B. Hastings, Entropy and entanglement in quantum ground states, *Phys. Rev. B* **76** (2007) 035114.
- [17] T.J. Osborne, M.A. Nielsen, Entanglement in a simple quantum phase transition, *Phys. Rev. A* **66** (2002) 032110.
- [18] L.-A. Wu, M.S. Sarandy, D.A. Lidar, Quantum phase transitions and bipartite entanglement, *Phys. Rev. Lett.* **93** (2004) 250404.
- [19] T.R. de Oliveira, G. Rigolin, M.C. de Oliveira, E. Miranda, Multipartite entanglement signature of quantum phase transitions, *Phys. Rev. Lett.* **97** (2007) 170401.
- [20] S.-J. Gu, H.-Q. Lin, Y.-Q. Li, Entanglement, quantum phase transition, and scaling in the XXZ chain, *Phys. Rev. A* **68** (2003) 042330.
- [21] J. Ren, X.-F. Xu, L.-P. Gu, J.-L. Li, Quantum information analysis of quantum phase tran-

- sitions in a one-dimensional  $V_1$ - $V_2$  hard-core-boson model, *Phys. Rev. A* **86** (2012) 064301.
- [22] M. Azuma, Z. Hiroi, M. Takano, K. Ishida, Y. Kitaoka, Observation of a spin gap in  $\text{SrCu}_2\text{O}_3$  comprising spin-1/2 quasi-1D two-leg ladders, *Phys. Rev. Lett.* **73** (1994) 3463.
- [23] T. Imai, K.R. Thurber, K.M. Shen, A.W. Hunt, F.C. Chou,  $^{17}\text{O}$  and  $^{63}\text{Cu}$  NMR in undoped and hole doped  $\text{Cu}_2\text{O}_3$  two-leg spin ladder  $\text{A}_{14}\text{Cu}_{24}\text{O}_{41}$  ( $\text{A}_{14}=\text{La}_6\text{Ca}_8, \text{Sr}_{14}, \text{Sr}_{11}\text{Ca}_3$ ), *Phys. Rev. Lett.* **81** (1998) 220.
- [24] G. Chaboussant, Experimental phase diagram of  $\text{Cu}_2(\text{C}_5\text{H}_{12}\text{N}_2)_2\text{Cl}_4$ : A quasi-one-dimensional antiferromagnetic spin-Heisenberg ladder, *Phys. Rev. B* **55** (1997) 3046.
- [25] E. Dagotto, T.M. Rice, Surprises on the way from one- to two-dimensional quantum magnets: The ladder materials, *Science* **271** (1996) 618-623.
- [26] B. Frischmuth, S. Haas, G. Sierra, T.M. Rice, Low-energy properties of antiferromagnetic spin-1/2 Heisenberg ladders with an odd number of legs, *Phys. Rev. B* **55** (1997) R3340.
- [27] D.C. Johnston, J.W. Johnson, D.P. Goshorn, A.J. Jacobson, Magnetic susceptibility of  $(\text{VO})_2\text{P}_2\text{O}_7$ : A one-dimensional spin-1/2 Heisenberg antiferromagnet with a ladder spin configuration and a singlet ground state, *Phys. Rev. B* **35** (1987) 219.
- [28] B. Frischmuth, B. Ammon, M. Troyer, Susceptibility and low-temperature thermodynamics of spin-1/2 Heisenberg ladders, *Phys. Rev. B* **54** (1996) R3714.
- [29] S. Fujiyama, M. Tikigawa, N. Motoyama, H. Eisaki, S. Uchida, Nuclear spin relaxation in hole-doped two-leg ladders, *J. Phys. Soc. Jpn.* **69** (2000) 1610-1613.
- [30] F. Neaf, X. Wang, Nuclear spin relaxation rates in two-leg spin ladders, *Phys. Rev. Lett.* **84** (2000) 1320.
- [31] X.Q. Wang, L. Yu, Magnetic-field effects on two-leg Heisenberg antiferromagnetic ladders: Thermodynamic properties, *Phys. Rev. Lett.* **84** (2000) 5399.
- [32] J. Vannimenus, G. Toulouse, Theory of the frustration effect. II. Ising spins on a square lattice, *J. Phys. C: Solid State Phys.* **10** (1977) L537.
- [33] D.S. Almeida, R.R. Montenegro-Filho, Quantum bicritical point and phase separation in a frustrated Heisenberg ladder, *Phys. Rev. B* **108** (2023) 224433.
- [34] S. Bose, Quantum communication through an unmodulated spin chain, *Phys. Rev. Lett.* **91** (2003) 207901.
- [35] J. Kurmann, H. Thomas, G. Müller, Antiferromagnetic long-range order in the anisotropic quantum spin chain, *Physica A* **112** (1982) 235-255.

- [36] L.C. Venuti, C.D.E. Boschi, M. Roncaglia, Long-distance entanglement in spin systems, *Phys. Rev. Lett.* **96** (2006) 247206.
- [37] S. Sahling, G. Remenyi, C. Paulsen, P. Monceau, V. Saligrama, C. Marin, A. Revcolevschi, L.P. Regnault, S. Raymond, J.E. Lorenzo, Experimental realization of long-distance entanglement between spins in antiferromagnetic quantum spin chains, *Nat. Phys.* **11** (2015) 255-260.
- [38] D.I. Bazhanov, I.N. Sivkov, V.S. Stepanyuk, Engineering of entanglement and spin state transfer via quantum chains of atomic spins at large separations, *Sci. Rep.* **8** (2018) 14118.
- [39] G. Gualdi, S.M. Giampaolo, F. Illuminati, Modular entanglement, *Phys. Rev. Lett.* **106** (2011) 050501.
- [40] S.M. Giampaolo, F. Illuminati, Long-distance entanglement in many-body atomic and optical systems, *New J. Phys.* **12** (2010) 025019.
- [41] J. Chen, K.-L. Yao, L.-J. Ding, Identification of intrinsic gapped behavior in spin-1/2 ladder with staggered dimerization, *Physica A* **391** (2012) 2306-2312.
- [42] X.-Y. Deng, L.-J. Kong, L. Qiang, String order and degenerate entanglement spectrum of  $S = 1/2$  and  $S = 1$  Heisenberg bond-alternating chains, *Eur. Phys. J. B* **87** (2014) 247.
- [43] S. Wessel, S. Haas, Three-dimensional ordering in weakly coupled antiferromagnetic ladders and chains, *Phys. Rev. B* **62** (2000) 316.
- [44] T. Kariyado, Y. Hatsugai, Topological order parameters of the spin-1/2 dimerized Heisenberg ladder in magnetic field, *Phys. Rev. B* **91** (2015) 214410.
- [45] C. Ding, Phase transitions and critical behaviors of XXZ ladders, *J. Stat. Mech. Theory Exp.* **2020** (2020) 013102.
- [46] L.-Z. Hu, Y.-L. Xu, P.-P. Zhang, S.-W. Yan, X.-M. Kong, Long-distance entanglement in antiferromagnetic XXZ spin chain with alternating interactions, *Physica A* **607** (2022) 128170.
- [47] R.-X. Li, S.-L. Wang, Y. Ni, K.-L. Yao, H.-H. Fu, 0- and 2/3-magnetization plateaus in three-leg antiferromagnetic Heisenberg spin-1/2 ladders with leg-dimerization, *Phys. Lett. A* **378** (2014) 970-974.
- [48] R.C. Aléio, M.L. Lyra, J. Strečka, Ground states, magnetization plateaus and bipartite entanglement of frustrated spin-1/2 Ising-Heisenberg and Heisenberg triangular tubes, *J. Magn. Magn. Mater.* **417** (2016) 294-301.
- [49] M. Greiter, H. Schmidt, Magnetic excitations in the site-centered stripe phase: Spin-wave theory of coupled three-leg ladders, *Phys. Rev. B* **83** (2011) 144422.

- [50] S.J. Gibson, R. Meyer, G.Y. Chitov, Numerical study of critical properties and hidden orders in dimerized spin ladders, *Phys. Rev. B* **83** (2011) 104423.
- [51] M. Azzouz, K. Shahin, G.Y. Chitov, Spin-Peierls instability in the spin-1/2 Heisenberg three-leg ladder, *Phys. Rev. B* **76** (2007) 132410.
- [52] X. Wang, N. Zhu, C. Chen, Ground-state phase diagram of a spin-1/2 frustrated three-leg antiferromagnetic Heisenberg ladder, *Phys. Rev. B* **66** (2002) 172405.
- [53] S. Wang, S. Zhu, Y. Ni, L. Peng, R. Li, K. Yao, Quantum phase transition and magnetic plateau in three-leg antiferromagnetic Heisenberg spin ladder with unequal  $J_1$ - $J_2$ - $J_1$  legs, *J. Magn. Magn. Mater.* **397** (2016) 319–324.
- [54] S.R. White, Density matrix formulation for quantum renormalization groups, *Phys. Rev. Lett.* **69** (1992) 2863.
- [55] L. Hulthén, Über das austauschproblem eines kristalls, *Ark. Mat. Astron. Fysik*, **26A** (1938) 1-106.
- [56] W.K. Wootters, Entanglement of formation of an arbitrary state of two qubits, *Phys. Rev. Lett.* **80** (1998) 2245.
- [57] S.-W. Tsai, J.B. Marston, Density-matrix renormalization-group analysis of quantum critical points: Quantum spin chains, *Phys. Rev. B* **62** (2000) 5546.
- [58] N. Laflorencie, E.S. Sørensen, M.-S. Chang, I. Affleck, Boundary effects in the critical scaling of entanglement entropy in 1D systems, *Phys. Rev. Lett.* **96** (2006) 100603.
- [59] J.v. Neumann, *Mathematical foundations of quantum mechanics*, Princeton University Press, Princeton, 1996.
- [60] V. Vedral, M.B. Plenio, M.A. Rippin, P.L. Knight, Quantifying entanglement, *Phys. Rev. Lett.* **78** (1997) 2275.
- [61] C.H. Bennett, H.J. Bernstein, S. Popescu, B. Schumacher, Concentrating partial entanglement by local operations, *Phys. Rev. A* **53** (1996) 2046.